RESTRICTED

NATIONAL ADVISORY COMMITTEE FOR AERONAUTICS

TECHNICAL NOTE

No. 975

DATA ON MATERIAL PROPERTIES AND PANEL COMPRESSIVE STRENGTH OF A PLASTIC-BONDED MATERIAL OF GLASS CLOTH AND CANVAS

By George W. Zender, Evan H. Schuette, and Robert A. Weinberger

Langley Memorial Aeronautical Laboratory
Langley Field, Va.

Washington
December 1944

RESTRICTED

NATIONAL ADVISORY COMMITTEE FOR AERONAUTICS

TECHNICAL NOTE NO. 975

DATA ON MATERIAL PROPERTIES AND PANEL COMPRESSIVE STRENGTH OF A PLASTIC-BONDED MATERIAL OF GLASS CLOTH AND CANVAS

By George W. Zender, Evan H. Schuette, and Robert A. Weinberger

SUMMARY

Results are presented of tests for determining the tensile, compressive, and bending properties of a material of plastic-bonded glass cloth and canvas layers. In addition, 10 panel specimens were tested in compression.

Although the material is not satisfactory for primary structural use in aircraft when compared on a strength-weight basis with other materials in common use, there appears to be potential strength in the material that will require research for development. These points are considered in some detail in the concluding discussion of the report.

An appendix shows that a higher tensile strength can be obtained by changes in the type of weave used in the glass-cloth reinforcement.

INTRODUCTION

Various plastic materials have been proposed for structural use in aircraft. In order to make use of such materials, tests must be made to determine their properties and to establish allowable stress values. This report presents the results of compression tests of 10 stiffened panels made of a plastic-bonded cloth material and tension, compression, and bending tests of enlarged samples of the same material. The specimens were furnished by the Virginia Lincoln Corp., Aircraft Division, Marion, Va.

DESCRIPTION OF MATERIAL

The plastic material tested, commercially known as "Valinite," consists of cloth layers impregnated and bonded with Plaskon 700 resin. In the panel specimens the two external layers were no. 162 Fiberglas fabric, whereas the internal layers were either no. 162 Fiberglas fabric or 8-ounce canvas. The material was furnished by the manufacturer in four compositions, which will be designated by their nominal percentages of glass cloth, as follows:

Nominal percentage of glass cloth (based on gross cross-sectional area)	Composition (layers)		Nominal thickness (in.)
	Glass	Canvas	
100	4	------	0.052
50	2	1	.052
$33\frac{1}{3}$	2	2	.078
25	2	3	.104

Some samples were also furnished that contained approximately the same percentages of glass cloth as the combinations just listed but had a larger total number of layers. The thicknesses of these samples were as follows:

Nominal percentage of glass cloth (based on gross cross-sectional area)	Thickness (in.)
100	0.661
50	.918
$33\frac{1}{3}$	.858
25	.629

Figure 1 shows the relative directions of the threads in the glass cloth and canvas for the specimens tested. For clarity, the threads that were more nearly straight are shown perfectly straight in figure 1, although actually there was some waviness in all threads.

In this report the direction along which the arrows are shown in figure 1 is designated the longitudinal direction, and the transverse direction is taken at right angles to it.

TEST SPECIMENS

Ten panel specimens, constructed of sheet and stiffeners of standard thickness, were tested in compression. Figure 2 shows the type of panel specimen and the symbols used for the dimensions; figure 3 shows one of these specimens after failure in the 1,200,000-pound-capacity testing machine in the NACA structures research laboratory. The specimen numbers, the composition, and the dimensions of the panels are given in table I. In specimens 150-1, 151-1, 151-2, and 152-1 the panel was assembled in such a manner that the load was applied along the transverse direction of the sheet. In the other specimens, the load was applied longitudinally. In almost all cases, the thread direction in the stiffeners was at an angle to the direction of loading.

In order to determine the longitudinal flexural rigidity and the longitudinal and transverse tensile and compressive properties of the material, specimens of standard shape were cut from the special oversize samples previously mentioned and were tested in the usual manner.

MATERIAL PROPERTIES

The results of the tests for determining tensile and compressive properties are given in figures 4 to 10, and the specimens after failure are shown in figures 11 to 14. A discussion of the effect of the composition of the material on the tension and compression moduli of elasticity is given in appendix A.

Figures 4 to 7 present stress-strain curves for the material. The ultimate stresses are plotted in figure 8. No ultimate stresses were recorded for two of the specimens because of difficulties in applying the load. The longitudinal tension specimen containing 100 percent glass was loaded by applying the grips against the edges of the cloth, and the pressure of the grips produced a separation of the cloth layers at a tensile stress of 21.4 kips per square inch. (See fig. 13.) Most of the other tension specimens were loaded by applying the grips against the surface of the cloth. With this method of loading, however, there was a large amount of slipping in the grips. In order to prevent this slipping, some of the specimens were loaded by applying the grips against the edges of the cloth and attaching plates, bolted together through the specimen, to the surfaces of the cloth to prevent separation of the layers. For the longitudinal specimen containing 25 percent glass, however, the bolt holes were evidently too large and failure occurred at one of these bolt holes at a tensile stress of 14.2 kips per square inch in the test section. (See fig. 13.)

The compression specimens that contained some canvas showed large increases in strain when a given load was left on for a period of time. Figures 9 and 10 show this increase, or creep, at various stresses as a function of time for the two compression specimens containing $33\frac{1}{3}$ percent glass.

The results of the bending tests are plotted in figure 15 and the bending specimens are shown after failure in figure 16. These specimens were tested as simple beams with concentrated loads applied at midspan. For this condition of loading, the deflection δ is given in inches by the equation

$$\delta = \frac{PL^3}{48EI} \tag{1}$$

where

P concentrated load at midspan, pounds

L length between end supports, inches

E bending modulus of elasticity, pounds per square inch

I moment of inertia of cross section, inches^4

The maximum fiber stress σ_{max} is given by the simple-bending formula

$$\sigma_{max} = \frac{Mc}{I} = \frac{\frac{PL}{4}\frac{h}{2}}{I} = \frac{PLh}{8I} \qquad (2)$$

where h is the depth of the beam. Eliminating P between equations (1) and (2) gives for the maximum fiber stress

$$\sigma_{max} = \frac{\delta}{\frac{L^2}{6h}}E$$

In figure 15, σ_{max} is plotted against the dimensionless quantity $\delta/(L^2/6h)$. The slope of the bending stress-strain curves therefore gives the value of the bending modulus of elasticity E.

PANEL SPECIMENS

Method of testing.- The ends of the panel specimens were ground flat, square, and parallel and were placed directly against the bearing plates of the testing machine. The specimens were alined by guide bars that extended across the bearing plates. These guide bars were moved away before the maximum load was reached to avoid interference with the action of the specimen at failure.

Strain gages were attached to both sides of each specimen on the stiffeners and between the stiffeners. The shortening of the specimens was also measured with dial gages.

Results.- The results of the panel tests are presented in figures 17 and 18 and in table I. Figure 17 shows the panel stress-strain curve for each of the specimens. In this figure, the stress plotted is the average stress on the panel and the strain is the total shortening of the panel divided by the length. Table I gives the ultimate load for each panel and the load at which separation occurred for the tests in which the stiffeners broke away from the panel.

In figure 18, the critical compressive stress for the sheet between stiffeners σ_{cr}, predicted from the strain-gage readings by the Southwell method as generalized in reference 1, is plotted against the ratio b/t_{skin} for each panel for which a prediction of the critical stress could be obtained.

Analysis of separation failure.- In some of the test panels, failure occurred by separation of the sheet from the stiffener. (See fig. 3.) This separation did not in general take place in the plane of the glued joint but within one of the thin wood veneers that were inserted between the sheet and stiffener. (See fig. 2.) When this type of failure occurred, it was observed that the sheet between stiffeners was in a buckled state.

An approximate theoretical analysis of a buckled plate, based on the theory of large deflections, revealed that, if separation occurs when the bending stress in the sheet adjacent to the stiffener reaches some constant failing value, the ratio of the edge stress to critical stress varies linearly with the reciprocal of the square of the critical stress and is equal to unity when this reciprocal is zero. This analysis assumes that the material is isotropic, that the edges of the plate are fixed, and that the relative shape of the buckle pattern is constant. Although the material in the panels was not isotropic, the sheet appeared to be essentially fixed to the stiffeners, the buckle patterns were always of the same relative shape, and the internal stress condition at which separation of sheet and stiffener occurred was probably a constant. The form of the theoretical solution for an isotropic material was therefore used to indicate the method of presenting test results.

The edge stress, or stress at the stiffener, was determined from strain-gage readings on the stiffener and the stress-strain curve for the material. The important values of edge stress are the values, designated σ_e, at which separation of the sheet from the stiffener occurred, or at which the panel failed without separation. The value of σ_e for failure without separation should be lower than the probable value of σ_e for separation.

In figure 19, values of σ_e/σ_{cr} are plotted against $1/\sigma_{cr}^2$. The straight line in figure 19 was drawn to conform with the theoretical analysis and indicates the probable values of separation stresses. The agreement seems reasonably good when the scatter that might be expected is considered. It will be noted that the point farthest from the straight line is for specimen 150-1, for which separation occurred in the plane of the glued joint; this deviation indicates that the glue did not hold so well as in the other specimens. The ultimate load for this specimen was also abnormally low. (See table I.)

CONCLUDING DISCUSSION

The stress-strain curves for material comprising 100 percent glass remain very nearly straight until failure, which occurs suddenly.

The stress-strain curves for specimens containing 25 percent, $33\frac{1}{3}$ percent, and 50 percent glass show appreciable yielding at stresses considerably below the maximum strength developed in the specimen containing 100 percent glass.

The fact that the tensile ultimate stresses are much higher both longitudinally and transversely than the corresponding compressive ultimate stresses indicates that the full strength of the material is probably not being realized in compression. This failure to realize the full strength may be caused by the waviness of the fibers in the glass cloth and canvas. Another possible reason for the low compressive strengths developed is that the compressive stress on the wavy fibers induces transverse forces that tend to rupture the plastic between layers of cloth and precipitate an early failure. A similar development of transverse forces between layers of cloth is present in tension tests but, as the fibers of glass and cloth straighten out, there is perhaps a tendency to approach more closely the potential strength of these fibers than is possible in compression tests. In any case, the waviness of the fibers and the weakness of the bonding agent are contributing factors in the low strengths developed. In appendix B, which was prepared after the main body of this report had been completed, it is shown that comparatively high tensile strengths are obtained by plastic-bonded unidirectional glass cloth.

The presence of canvas in the material causes large creep at loads considerably less than the maximum. The creep is, in fact, so large that further development of this type of material for primary structural uses should apparently be concentrated on the plastic reinforced with 100 percent glass.

The tests of stiffened panels indicate that the attachment of stiffeners to sheet through the medium of wood veneers is a point of weakness in the specimen. The strengths of the stiffened panels did follow theoretical laws, and practical design information could doubtless be obtained from the present background of experience in metal by making suitable tests of reinforced-plastic structural assemblies.

At present, the material is not good enough to compete on a strength-weight basis with aluminum alloys, which weigh 50 percent more but develop 400 percent more compressive strength. If the compressive strength could be appreciably increased, the plastic with 100-percent-glass reinforcement would be worthy of consideration for use in primary structural members of aircraft.

If a failure of the plastic bond between adjacent layers of cloth is responsible for the low compressive strength of the material, then an increase in this strength should be possible by some sort of reinforcement that would oppose the separation of the layers. Reinforcement of this type might be provided by forming a specimen as shown in figure 20. This type of specimen embodies the same principle as a spirally reinforced concrete column, for which much higher stresses are permitted than for an ordinary tied concrete column. Although it would perhaps not be possible to use directly the method of fabrication shown in figure 20 in the making of primary structural parts, tests of specimens of this type might assist in pointing the way to possible improvements in the material.

Langley Memorial Aeronautical Laboratory
National Advisory Committee for Aeronautics
Langley Field, Va., August 16, 1944

APPENDIX A

PREDICTION OF MODULUS OF ELASTICITY

The plastic material tested consists basically of two different types of fabric. If the modulus of elasticity of each of these fabrics is known, a prediction of the modulus of elasticity for any combination of the two fabrics should be possible.

In order to make such a prediction, the cross-sectional area of thread that is active in carrying load in each direction must be known. Measurements by optical micrometer were therefore taken of sample threads from each of the two fabrics. The areas of thread cross section found by this means and the observed number of threads per inch were as follows:

Thread	Area (sq in.)	Threads per inch
Longitudinal glass	0.000474	29
Transverse glass	.000391	15
Longitudinal canvas	.000350	27
Transverse canvas	.000172	74

The manufacturer lists the number of threads per inch in the Fiberglas fabric as 28 longitudinal and 16 transverse. The slight discrepancy between these and the measured values is probably caused by distortion of the cloth during fabrication of the specimens.

In a piece of glass cloth having a cross section 1 inch by 0.026 inch (two thicknesses), the total area of glass threads active in carrying load in the longitudinal direction is therefore

$$2 \times 29 \times 0.000474 = 0.02748 \text{ sq in.} \qquad (3)$$

In a piece of canvas of the same cross section (one thickness), the total area of canvas threads active in carrying load in the longitudinal direction is

$$27 \times 0.000350 = 0.00944 \text{ sq in.}$$

In each of the preceding cases, the total cross-sectional area of fabric is

$$1 \times 0.026 = 0.026 \text{ sq in.} \tag{4}$$

Equation (3) shows a larger area than equation (4) because the measurements of the threads were made after they had been removed from the cloth and were not confined by the surrounding threads.

If the percentage of glass in a given specimen is 100 p (p is then the percentage expressed decimally), and if the total cross-sectional area of the specimen is A, then the active area of glass in the longitudinal direction is

$$A_G = \frac{0.02748}{0.026} pA \tag{5}$$

and the active area of canvas is

$$A_C = \frac{0.00944}{0.026} (1 - p)A \tag{6}$$

If the load P is divided between the glass and canvas threads, P_G in the glass and P_C in the canvas, and if the glass threads have a modulus of elasticity E_G and the canvas threads have a modulus of elasticity E_C (the effect of the surrounding plastic material is neglected), the resulting strain ϵ is

$$\epsilon = \frac{P_G}{A_G E_G} = \frac{P_C}{A_C E_C} \tag{7}$$

From equation (7)

$$P_G = P_C \frac{A_G}{A_C} \frac{E_G}{E_C}$$

Now the total load P must be given by

$$P = P_C + P_G$$

$$= P_C\left(1 + \frac{A_G}{A_C}\frac{E_G}{E_C}\right) \qquad (8)$$

From equations (5) and (6)

$$\frac{A_G}{A_C} = 2.910\frac{p}{1 - p} \qquad (9)$$

From equations (6) and (7)

$$\epsilon = \frac{P_C}{AE_C}\frac{1}{0.363(1 - p)} \qquad (10)$$

The longitudinal modulus of elasticity E_L of the combined materials is given by the equation

$$E_L = \frac{P}{A\epsilon} \qquad (11)$$

Substitution of equations (8), (9), and (10) in equation (11) gives

$$E_L = \frac{P_C\left(1 + 2.910\frac{p}{1 - p}\frac{E_G}{E_C}\right)}{\frac{P_C}{E_C}\frac{1}{0.363(1 - p)}}$$

$$= 0.363(1 - p)E_C + 1.057pE_G \qquad (12)$$

Equation (12) gives the longitudinal modulus of elasticity for the material in terms of the two basic moduli E_C

and E_G and the nominal percentage of glass. A similar calculation gives for the transverse modulus of elasticity E_T in terms of the same basic moduli

$$E_T = 0.490(1 - p)E_C + 0.452pE_G$$

It is necessary to determine the basic moduli E_C and E_G. Figure 21 is a graph of the various directional moduli, in which the values of E_C and E_G were chosen to give the best fit with the experimental points. The values used are as follows:

Load	E_C (lb/sq in.)	E_G (lb/sq in.)
Compression	2.50×10^6	3.29×10^6
Tension	3.98×10^6	6.22×10^6

The experimental stress-strain curves showed no initial straight-line portion; secant moduli, taken at stresses of 1000 pounds per square inch in compression and 2500 pounds per square inch in tension, were therefore used in plotting the experimental points in figure 21.

When the errors in measuring and counting threads and inconsistencies within the material are considered, the agreement between experimental and calculated values in figure 21 seems good.

APPENDIX B

TENSILE TESTS OF PLASTIC-BONDED UNIDIRECTIONAL CLOTH

After the completion of the body of this report, tension tests were made of standard specimens cut from a thin sheet (seven layers, total thickness, 0.0834 in.) of plastic-bonded material of unidirectional glass cloth, which was also furnished by the Virginia Lincoln Corp., Aircraft Division. The type of weave used in this material is shown in figure 22.

The longitudinal and transverse tensile stress-strain curves obtained from the tests are shown in figure 23. Figure 24 shows the transverse stress-strain curve drawn to a larger scale.

The longitudinal tensile stress-strain curve remained relatively straight until failure, which occurred at a stress of 82.9 kips per square inch. The transverse strength of 1.77 kips per square inch is practically negligible by comparison with the longitudinal strength. Reasonably good tensile properties in both directions could probably be obtained, however, by cross-laminating the material.

No compression tests of this material were made.

REFERENCE

1. Lundquist, Eugene E.: Generalized Analysis of Experimental Observations in Problems of Elastic Stability. NACA TN No. 658, 1938.

TABLE I.- DIMENSIONS AND COMPRESSIVE STRENGTH OF STIFFENED PANELS

Specimen	Composition (a)		Approx. percentage of glass (a)	Length (in.)	Width (in.)	b (in.)	t_{stiff} (in.)	t_{skin} (in.)	Total area (sq in.)	Weight (lb)	Load (kips)		Average stress (kips/sq in.)	
	Glass	Canvas									Separation	Maximum	Separation	Maximum
153-1	4	0	100	24.56	18.15	1.62	0.054	0.066	2.50	3.36	-------	10.50	-------	4.20
150-2	2	1	50	24.91	18.25	1.68	.054	.056	2.35	3.03	9.95	9.95	4.23	4.23
150-3	2	1	50	24.86	22.70	3.14	.052	.051	2.49	3.31	10.43	10.43	4.20	4.20
150-1	2	1	50	24.79	28.60	5.17	.055	.058	3.10	3.76	7.73	8.46	2.50	2.73
151-3	2	2	$33\frac{1}{3}$	24.67	18.11	1.74	.083	.078	3.15	4.10	-------	14.50	-------	4.60
151-2	2	2	$33\frac{1}{3}$	24.62	22.63	3.34	.083	.082	3.70	4.55	-------	13.50	-------	3.65
151-1	2	2	$33\frac{1}{3}$	24.91	28.75	5.03	.080	.081	4.18	5.34	-------	15.00	-------	3.60
152-3	2	3	25	24.90	18.19	1.68	.101	.107	3.90	4.81	-------	14.18	-------	3.64
152-1	2	3	25	24.26	22.75	3.13	.110	.106	4.72	5.24	-------	16.50	-------	3.50
152-2	2	3	25	24.48	28.67	5.05	.107	.109	5.38	6.35	17.90	17.90	3.33	3.33

[a]Stiffeners and sheet have the same composition.

NATIONAL ADVISORY
COMMITTEE FOR AERONAUTICS

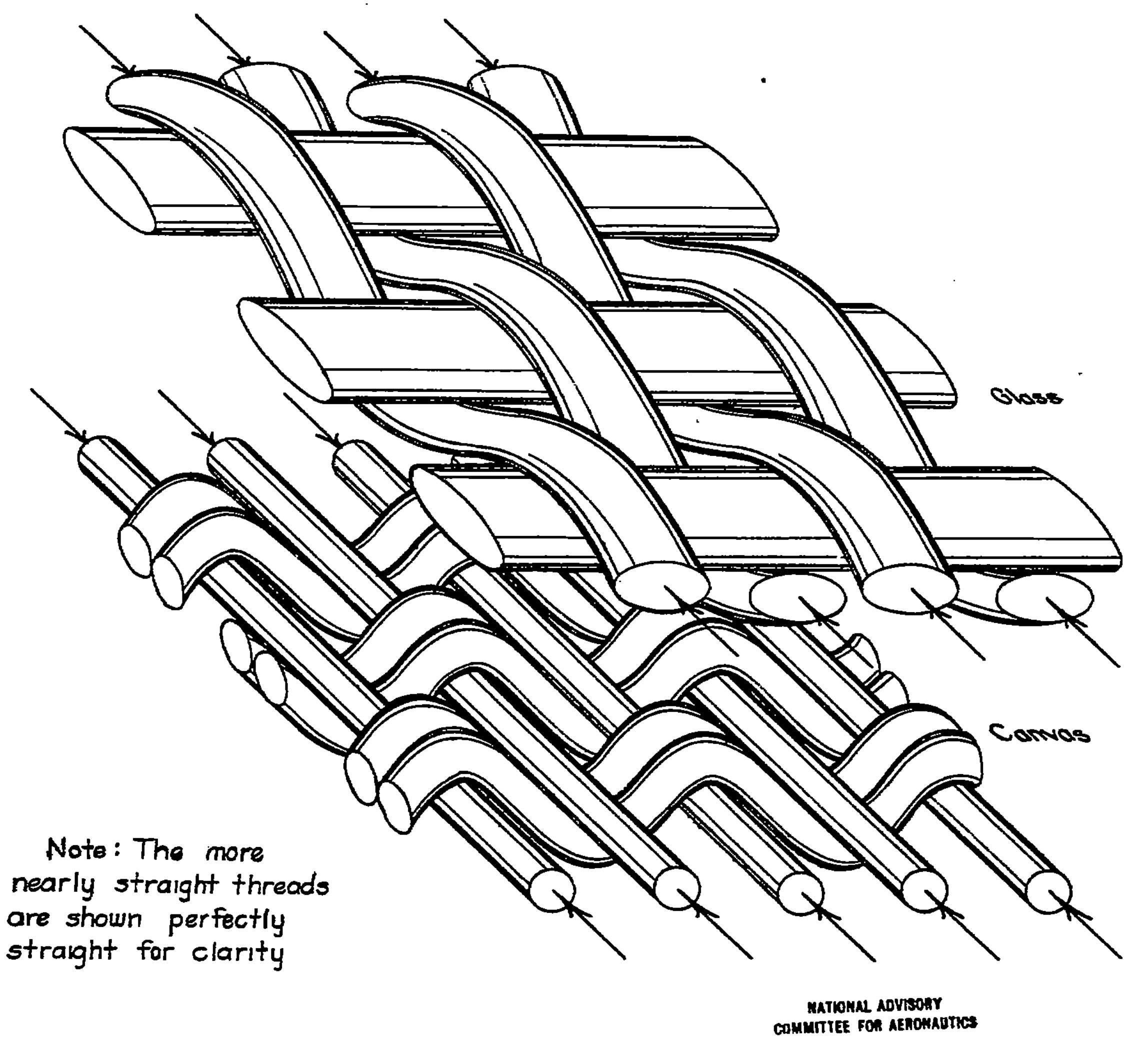

Figure 1.- Relative directions of threads in glass cloth and canvas. Arrows indicate longitudinal direction of loading.

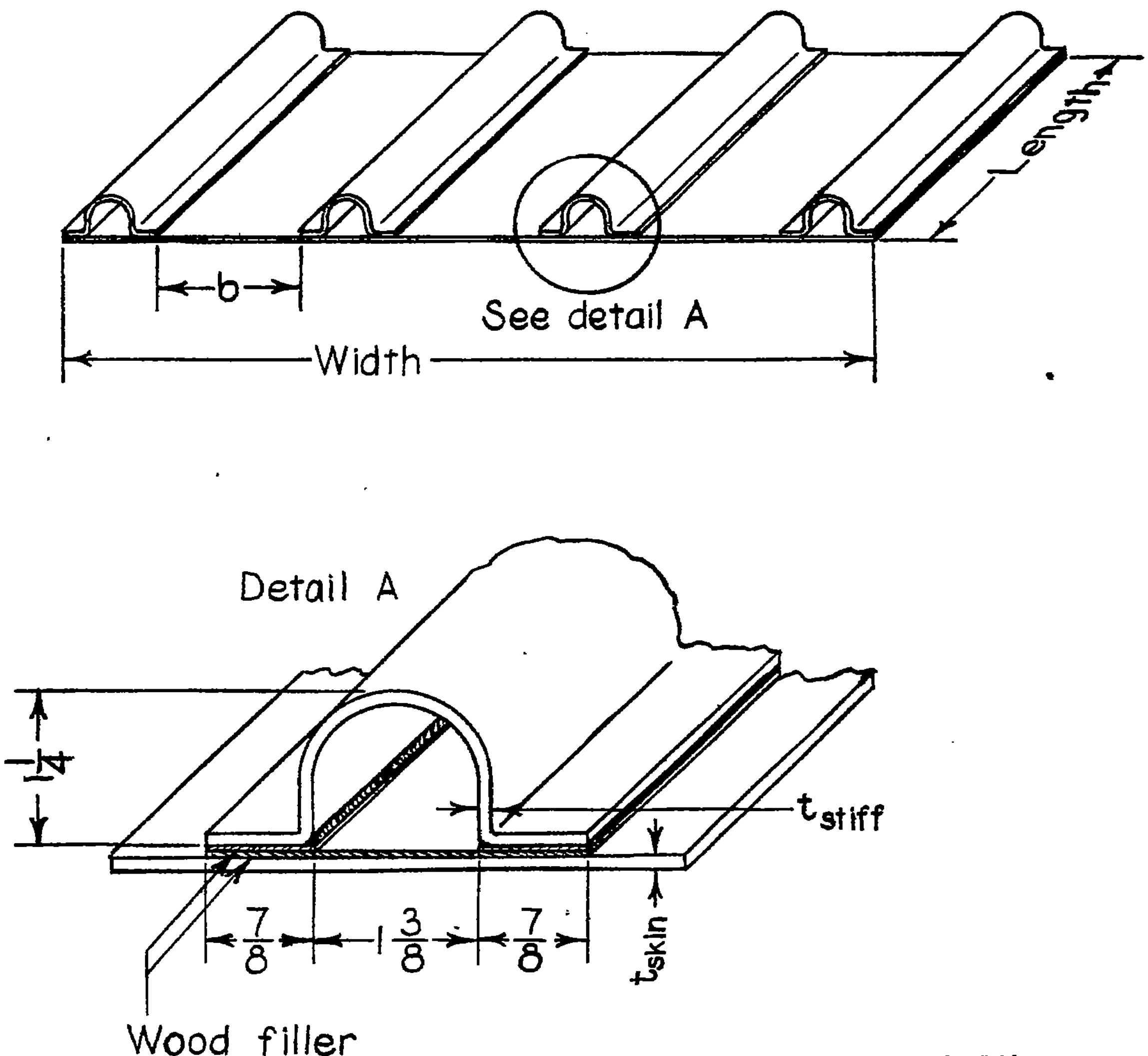

NATIONAL ADVISORY COMMITTEE FOR AERONAUTICS

Figure 2.- Sketch of test panel.

Figure 3.- Test panel after failure in testing machine.

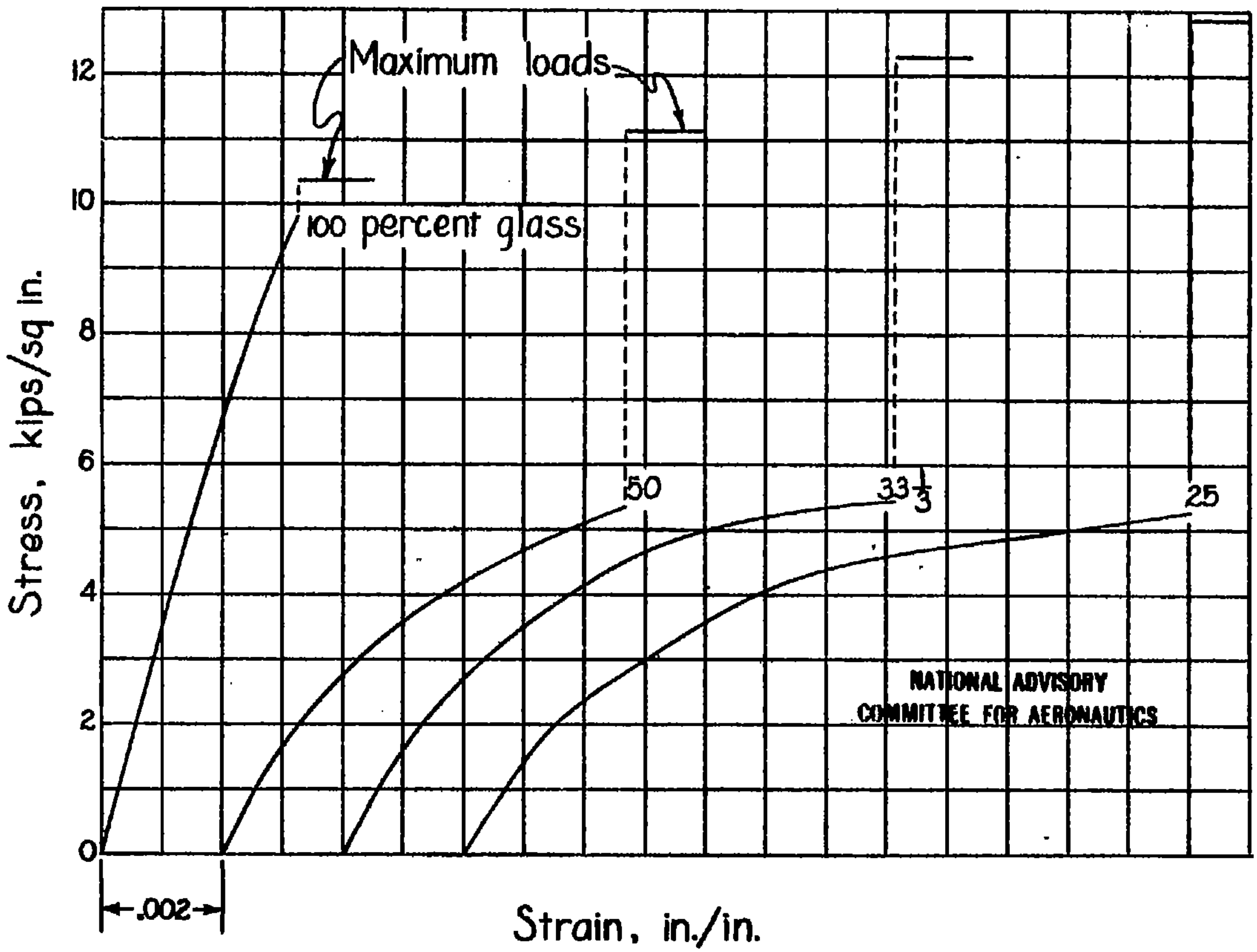

Figure 4.- Longitudinal compressive stress-strain curves.

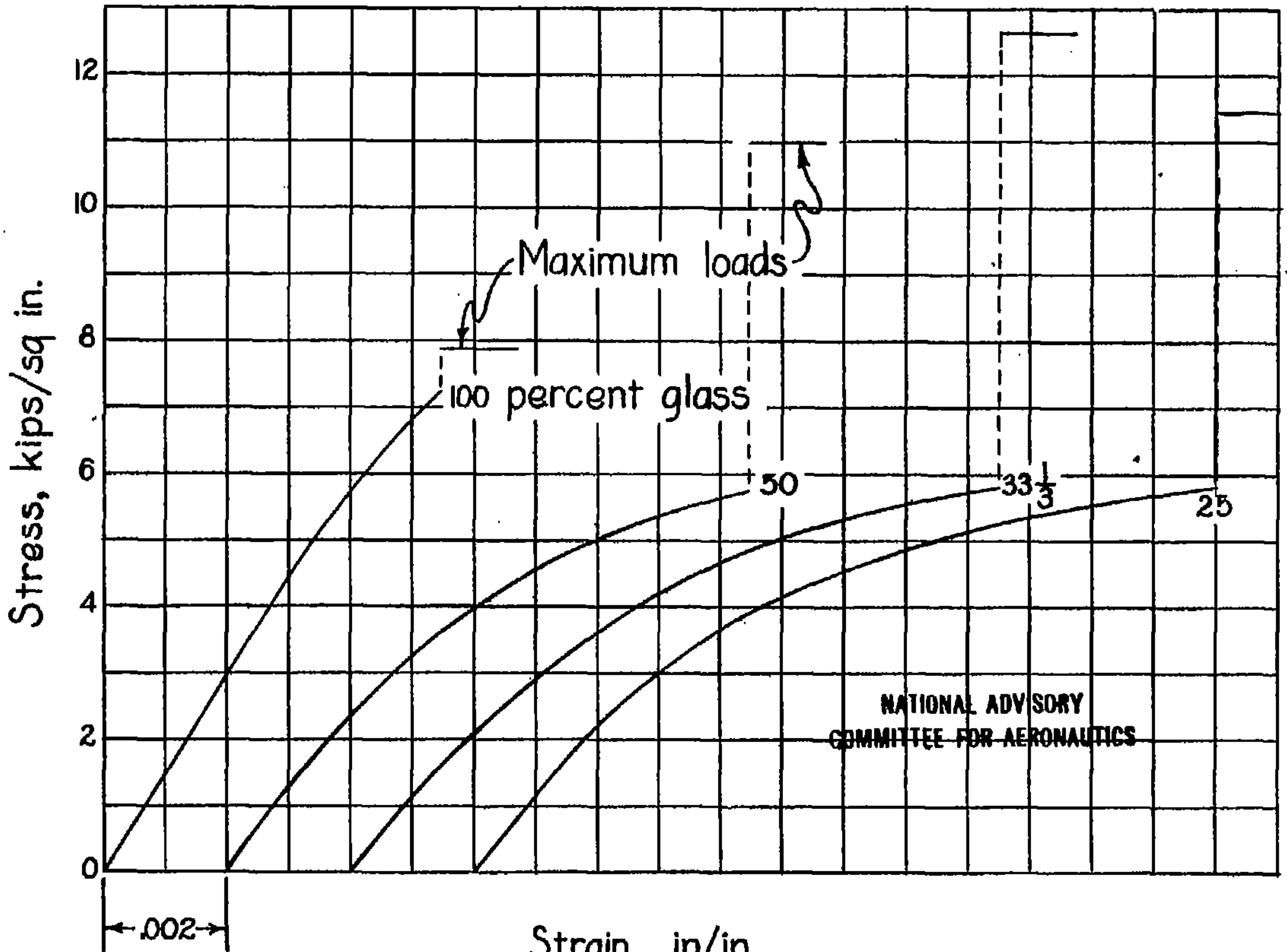

Figure 5.- Transverse compressive stress-strain curves.

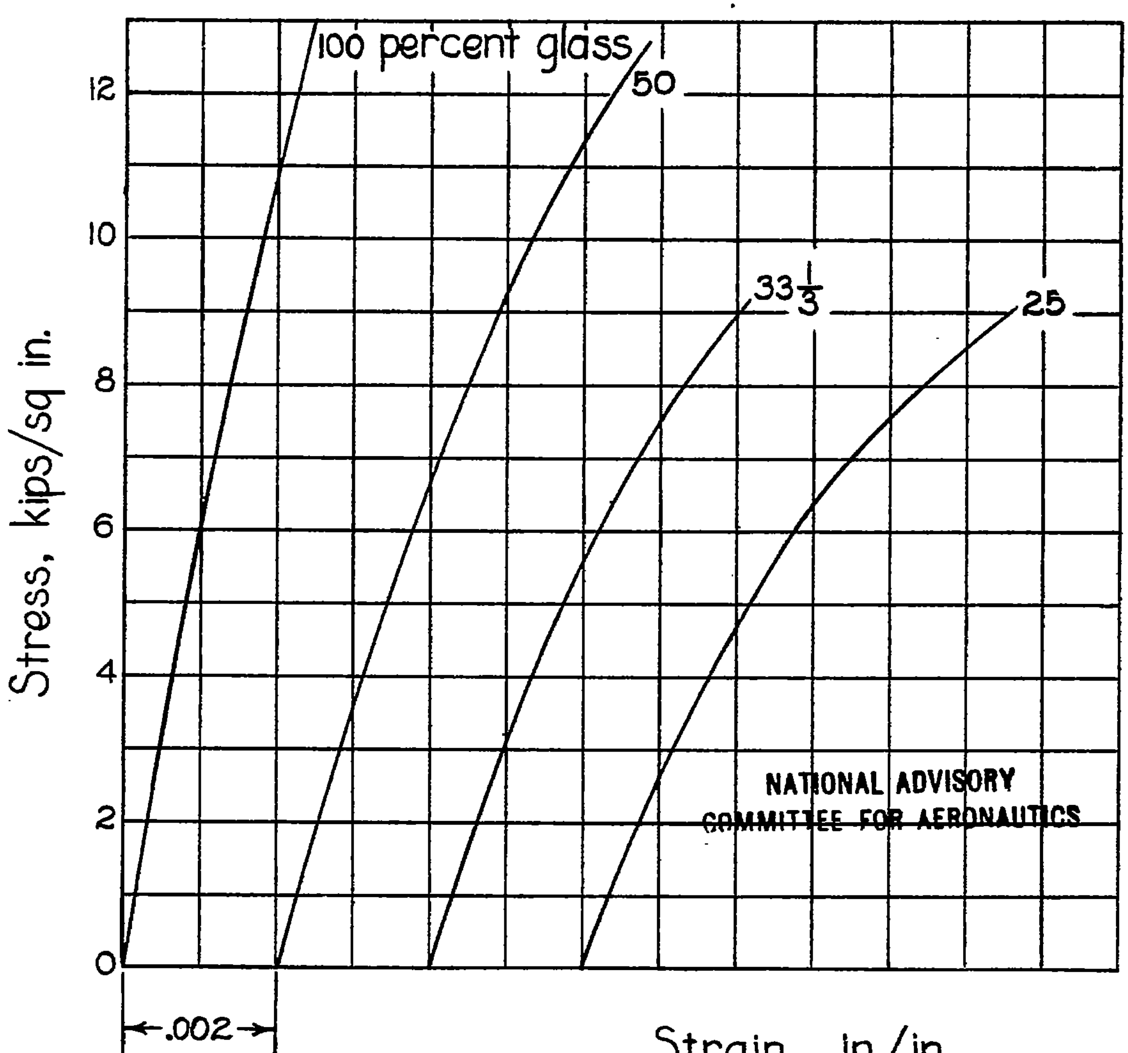

Figure 6.- Longitudinal tensile stress-strain curves.

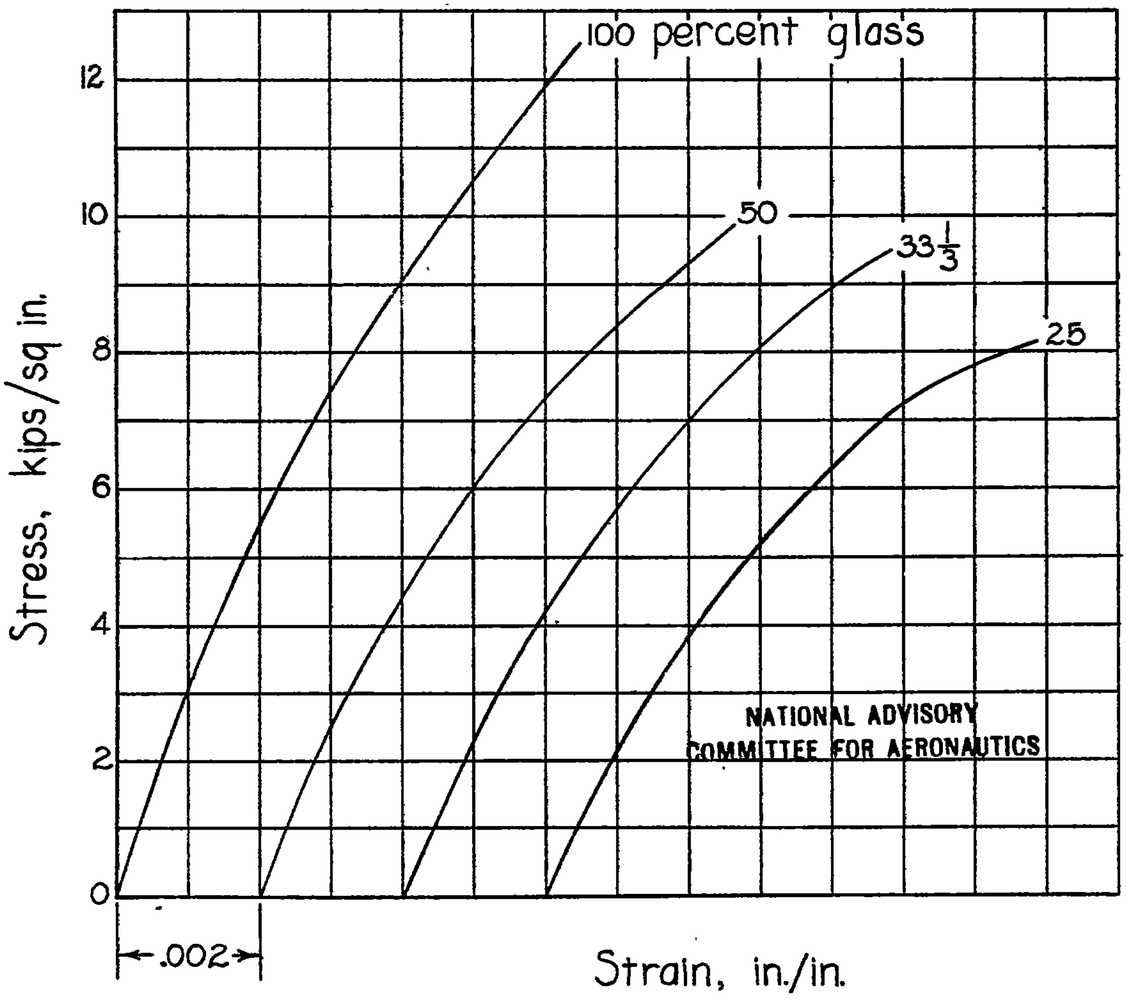

Figure 7. - Transverse tensile stress-strain curves.

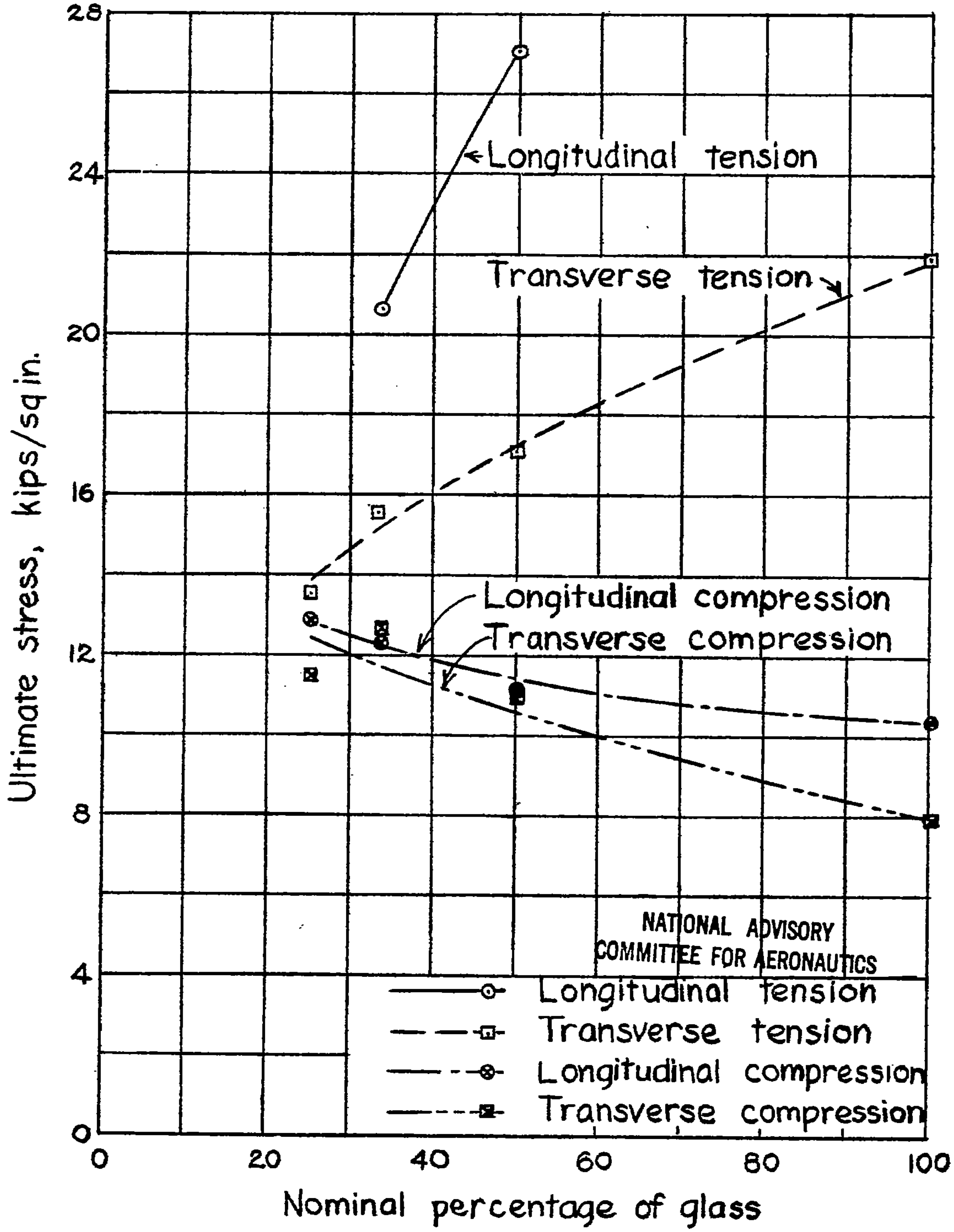

Figure 8.- Ultimate stresses for tension and compression specimens.

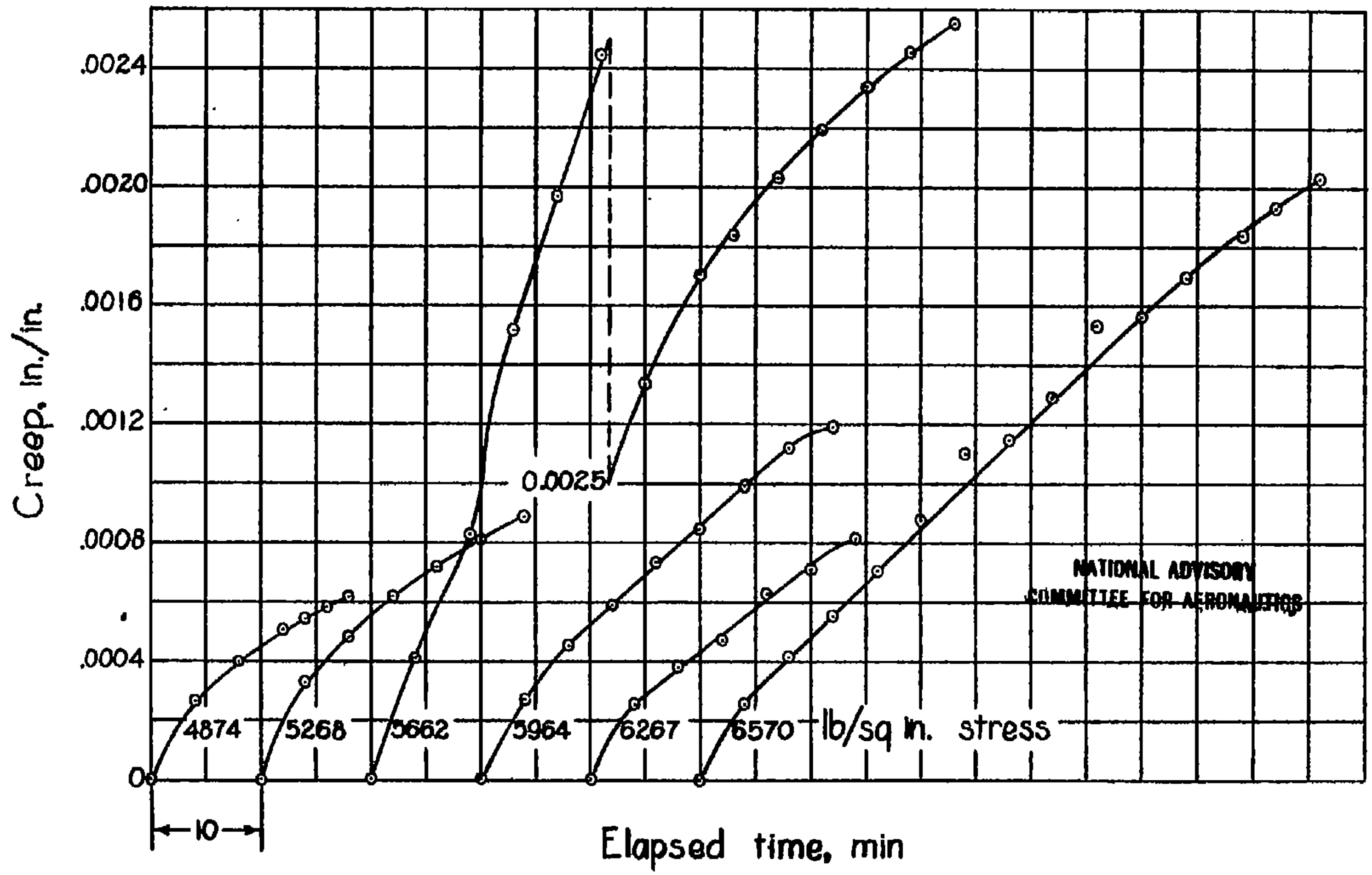

Figure 9.- Longitudinal compressive creep curves for $33\frac{1}{3}$ percent glass.

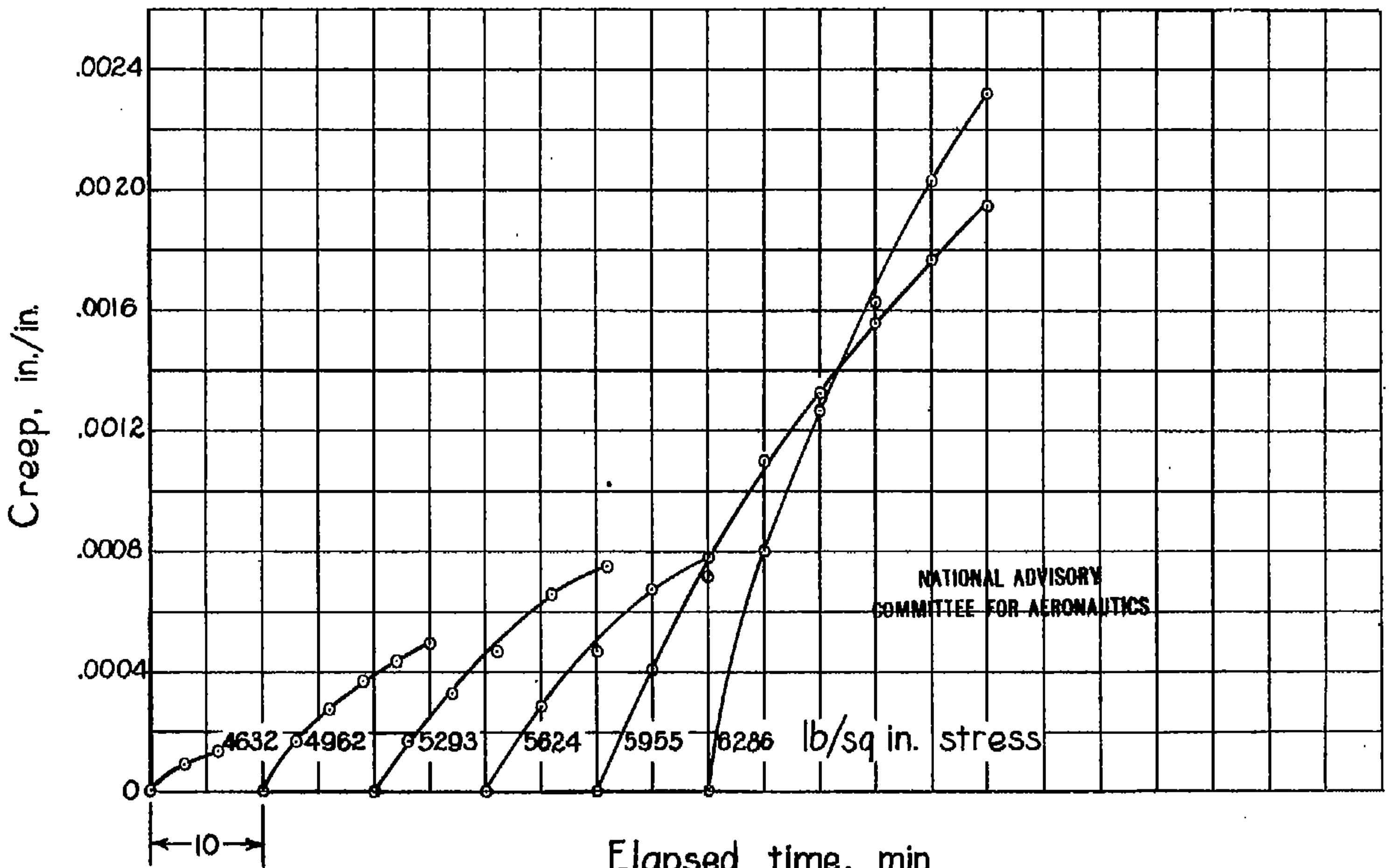

Figure 10.- Transverse compressive creep curves for $33\frac{1}{3}$ percent glass.

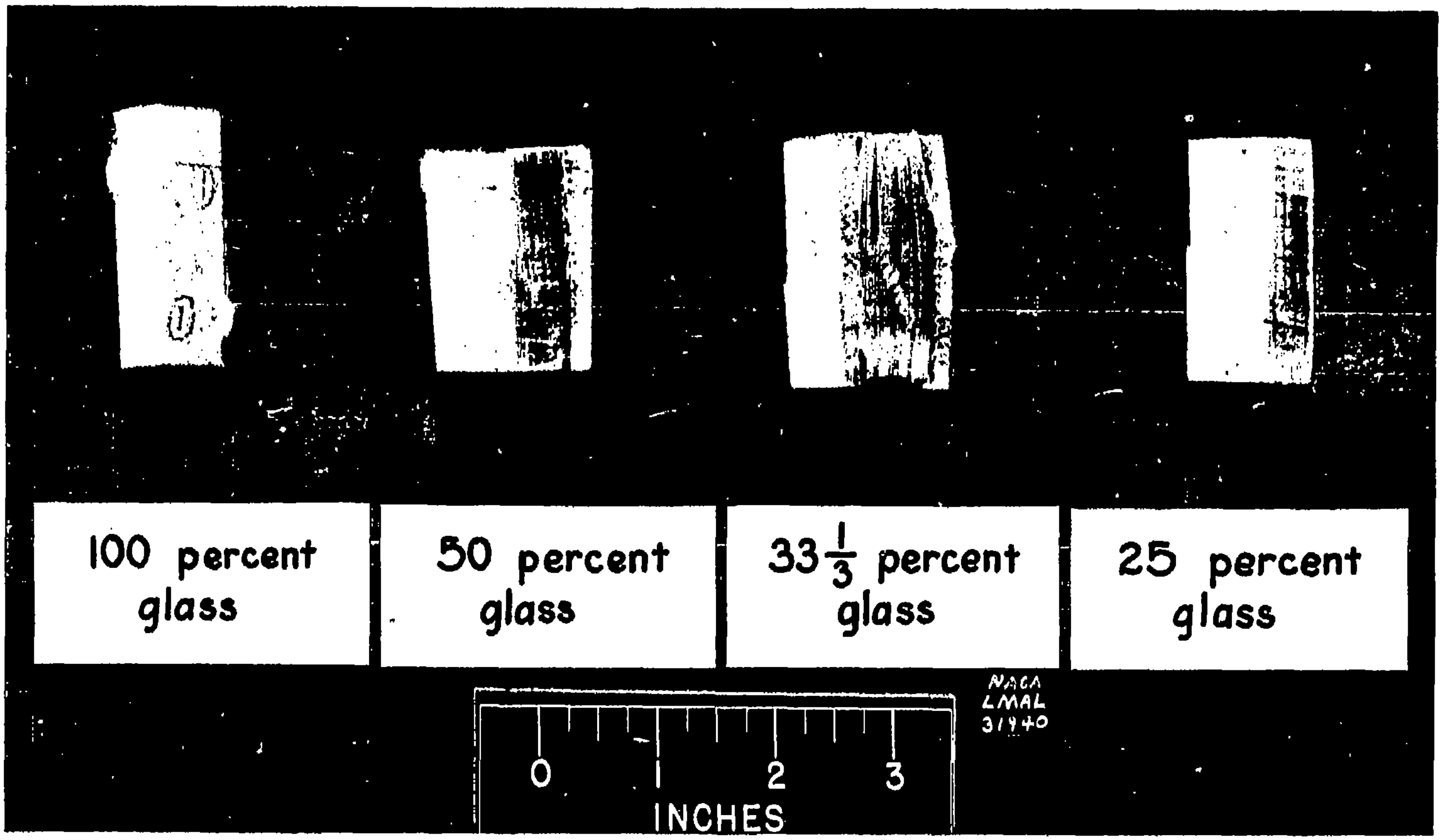

Figure 11.- Longitudinal compression specimens after failure.

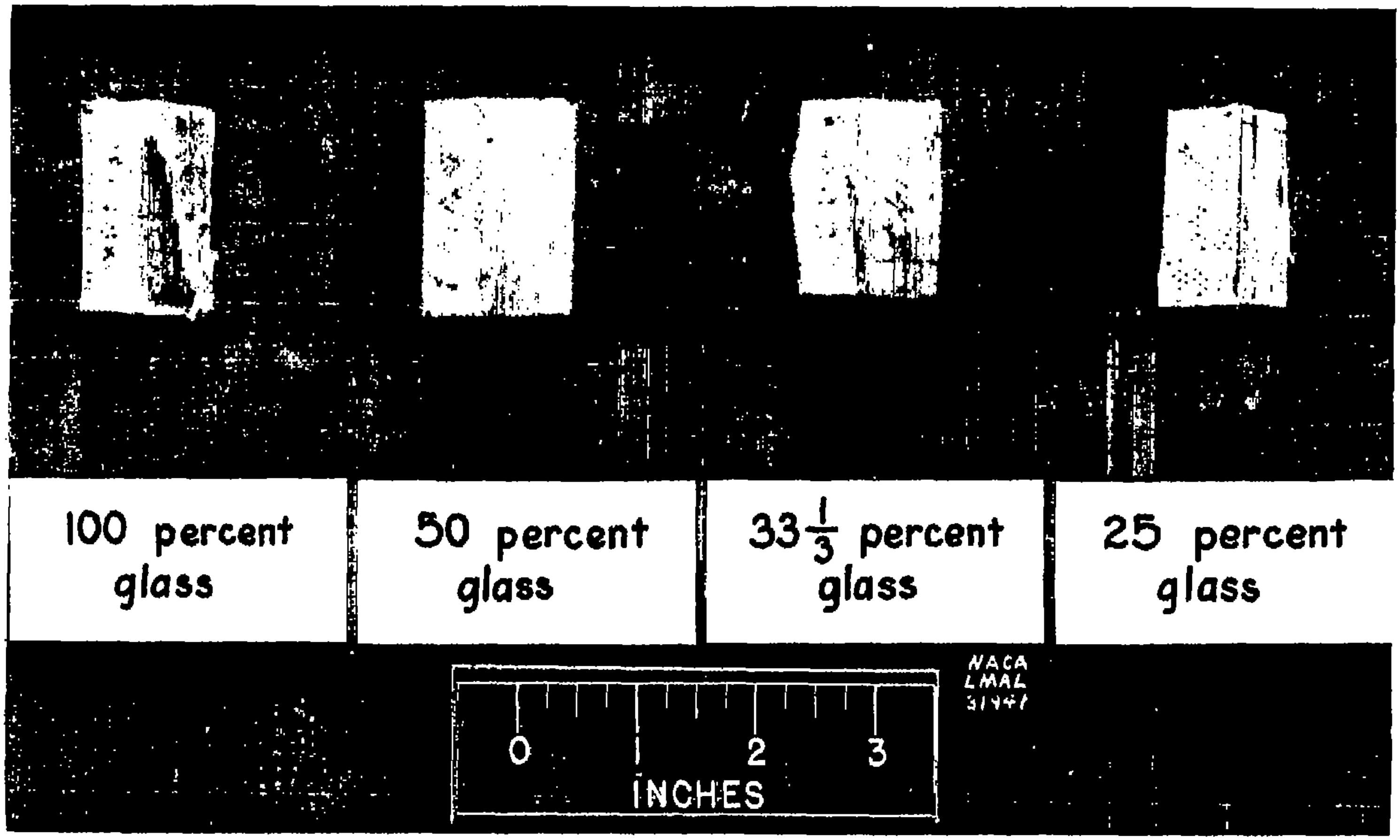

Figure 12.- Transverse compression specimens after failure.

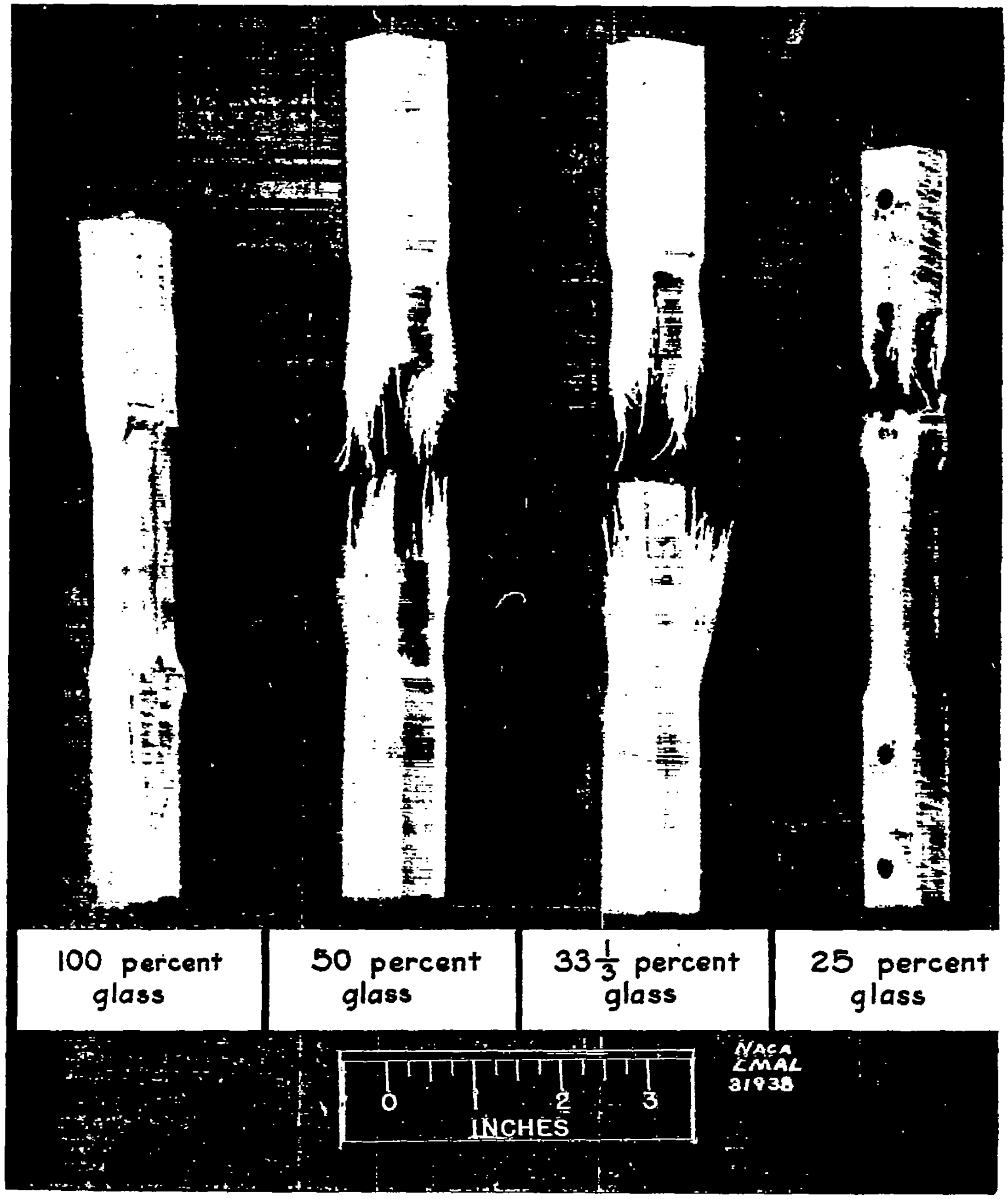

Figure 13.- Longitudinal tension specimens after failure.

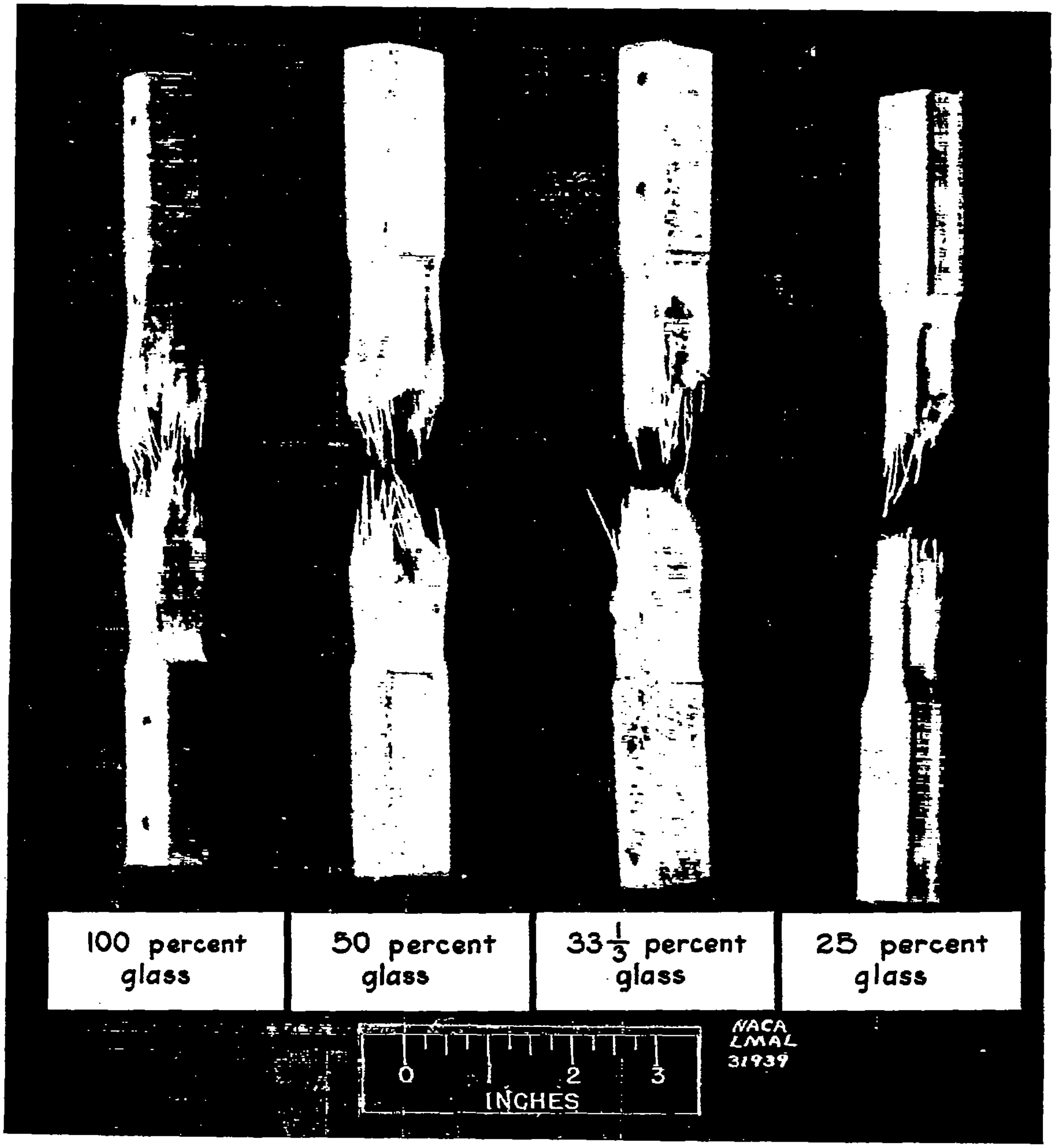

Figure 14.- Transverse tension specimens after failure.

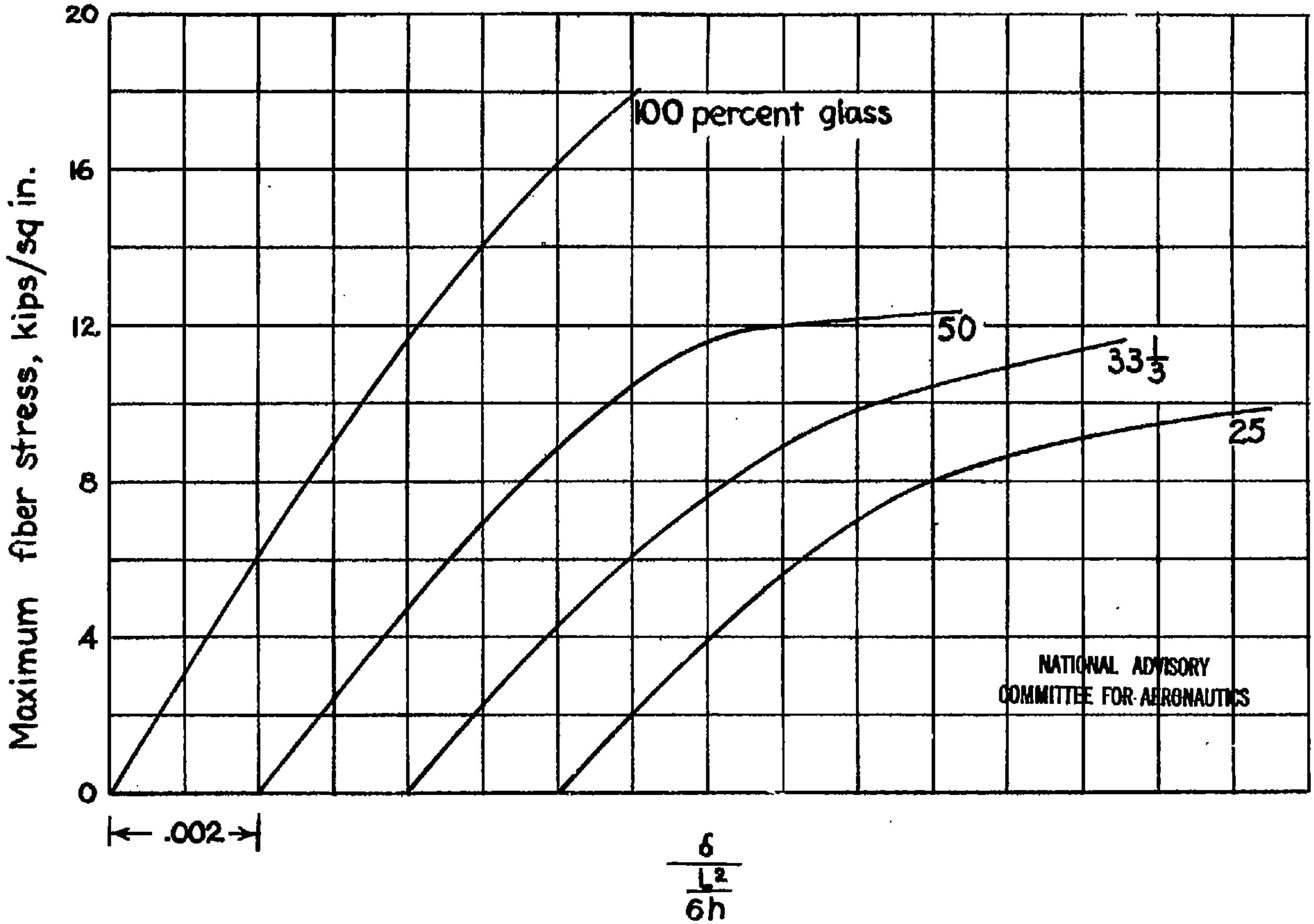

Figure 15.- Longitudinal bending stress-strain curves.

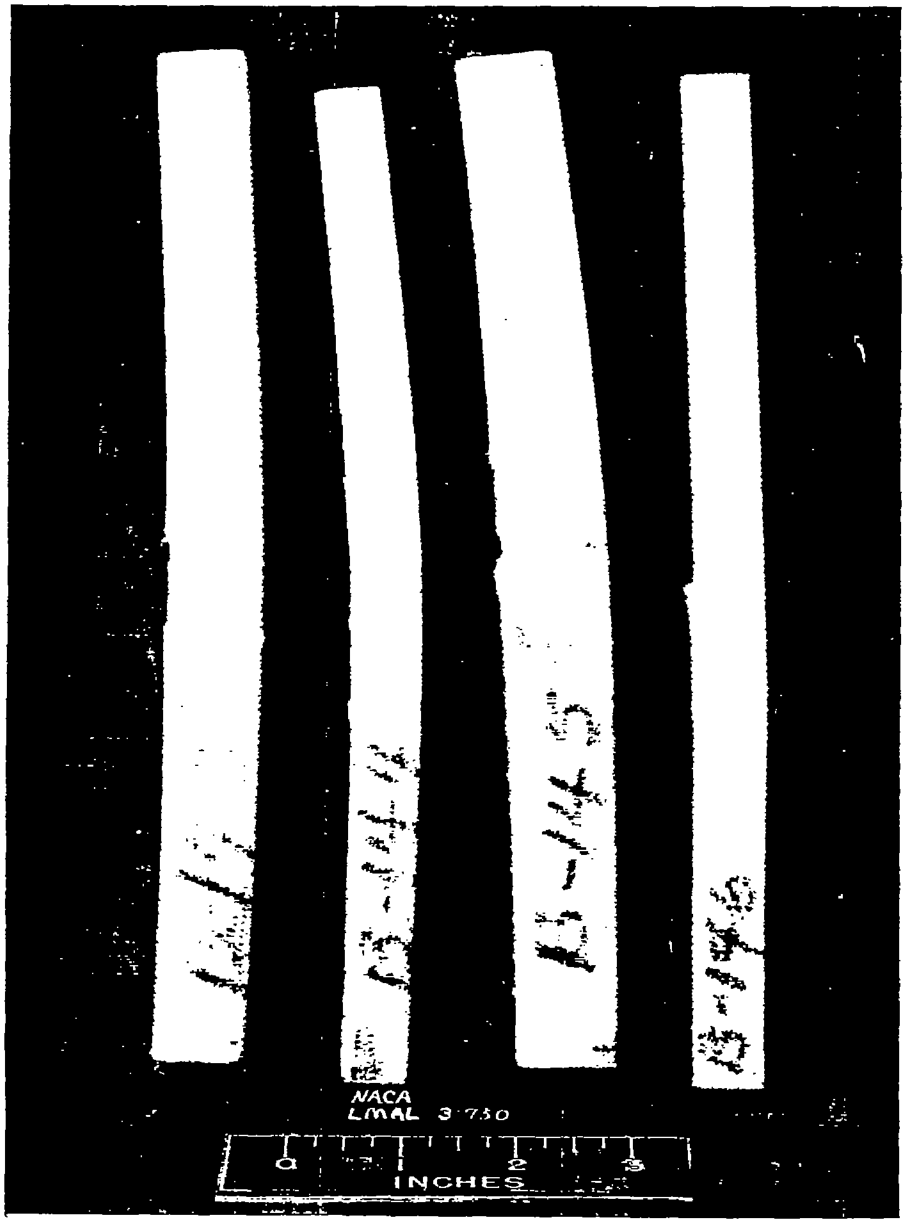

Figure 16.- Longitudinal bending specimens after failure. Left to right: $33\frac{1}{3}$, 25, 50, 100 percent glass.

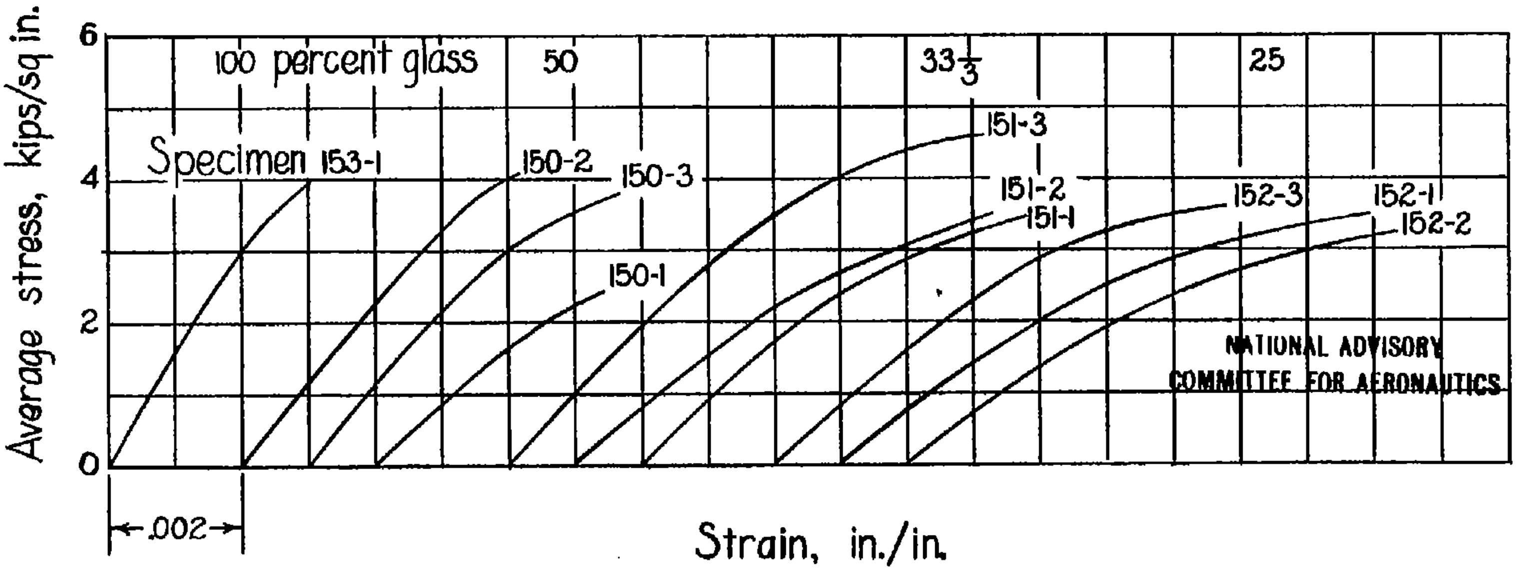

Figure 17. - Compressive panel stress-strain curves.

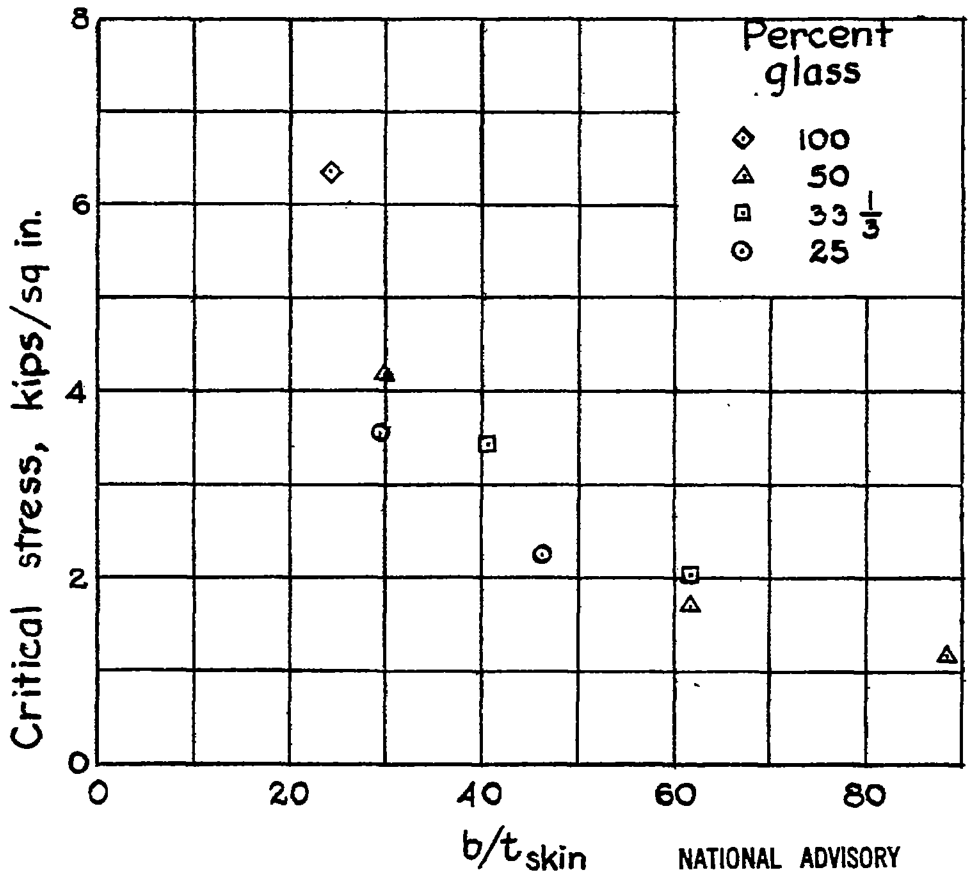

Figure 18.-Variation of critical compressive stress for sheet between stiffeners with b/t_{skin}.

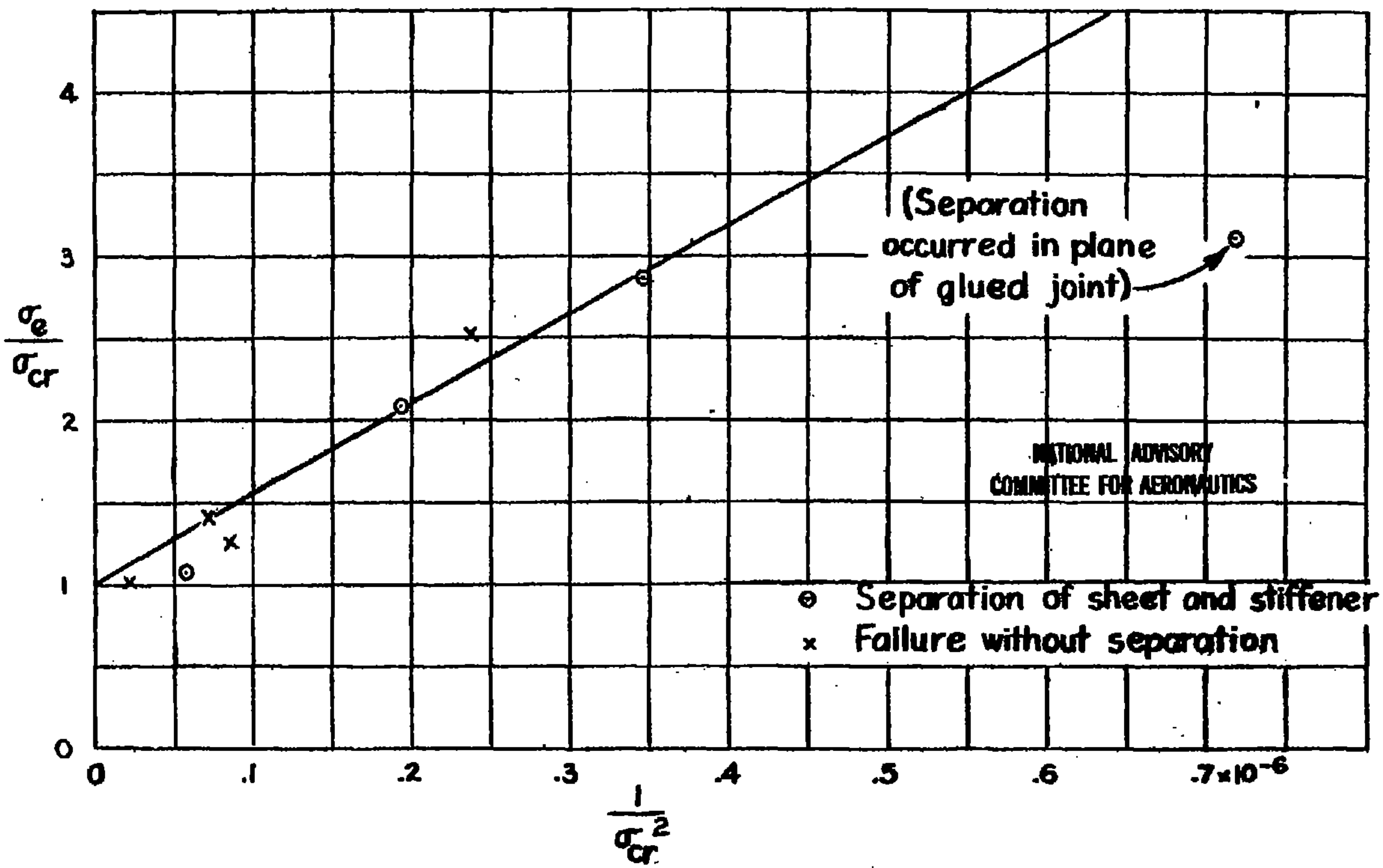

Figure 19.- Variation of σ_e/σ_{cr} with $1/\sigma_{cr}^2$.

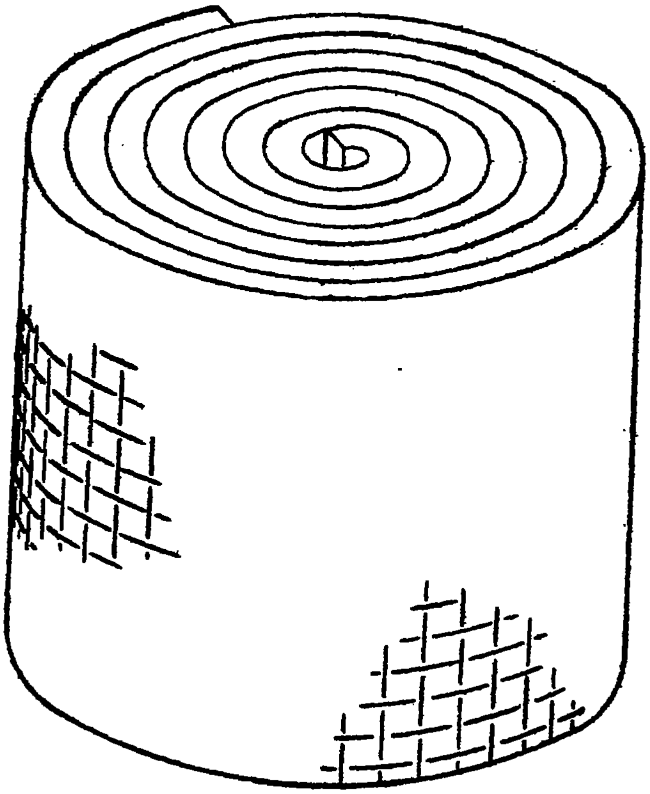

NATIONAL ADVISORY
COMMITTEE FOR AERONAUTICS

Figure 20.- Proposed type of compression specimen for studying effect of spiral reinforcing.

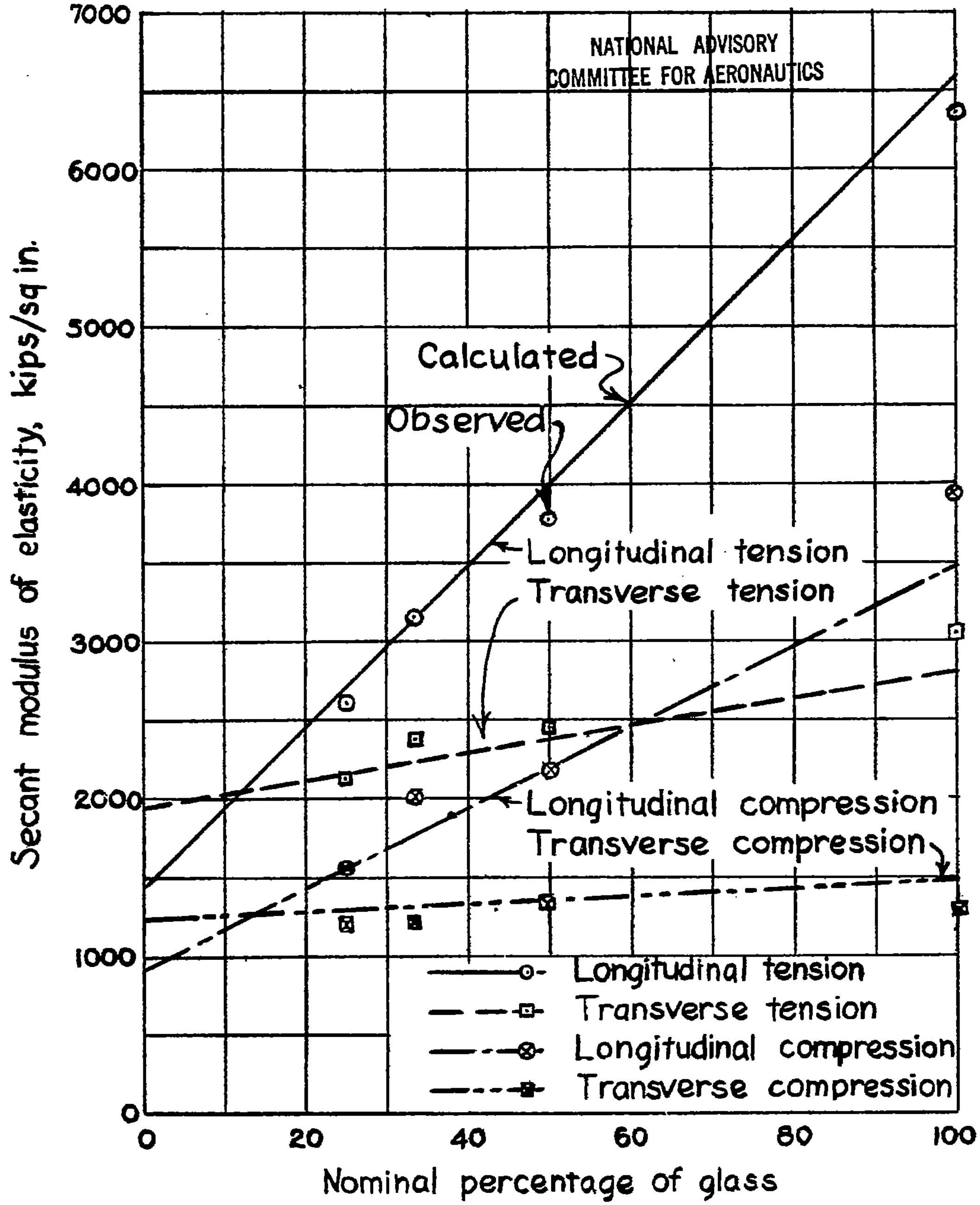

Figure 21. - Comparison of observed and calculated values of secant modulus of elasticity. Secant modulus taken at stresses of 1000 pounds per square inch in compression, 2500 pounds per square inch in tension.

NATIONAL ADVISORY
COMMITTEE FOR AERONAUTICS

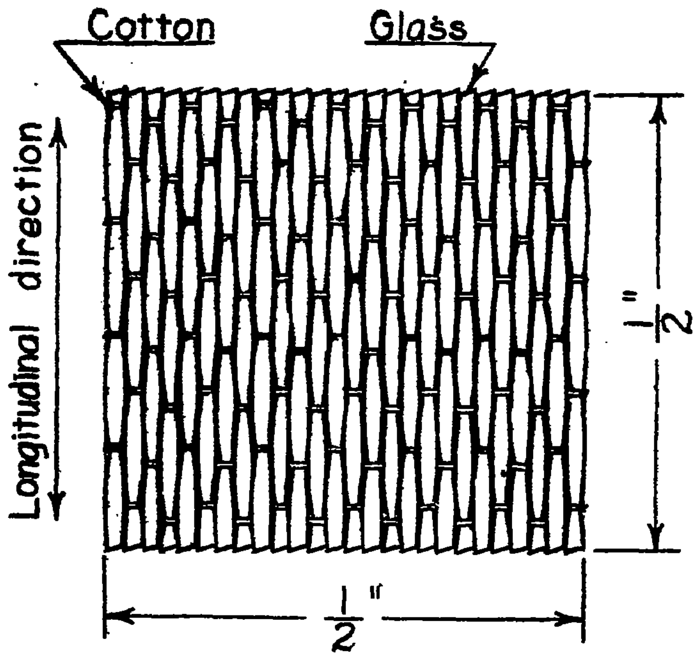

Figure 22.- Unidirectional fabric.

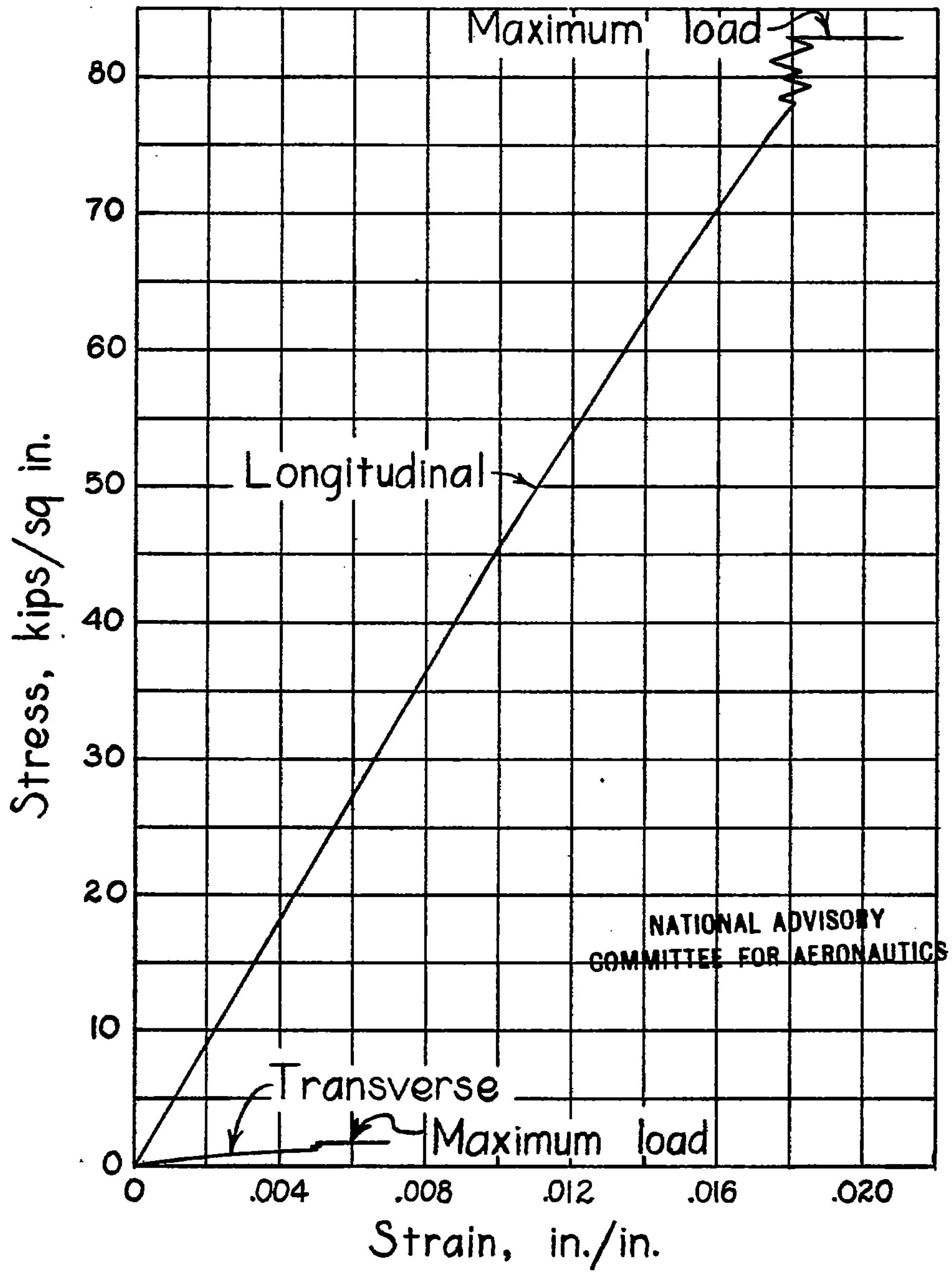

Figure 23. – Tensile stress-strain curves for plastic-bonded unidirectional cloth.

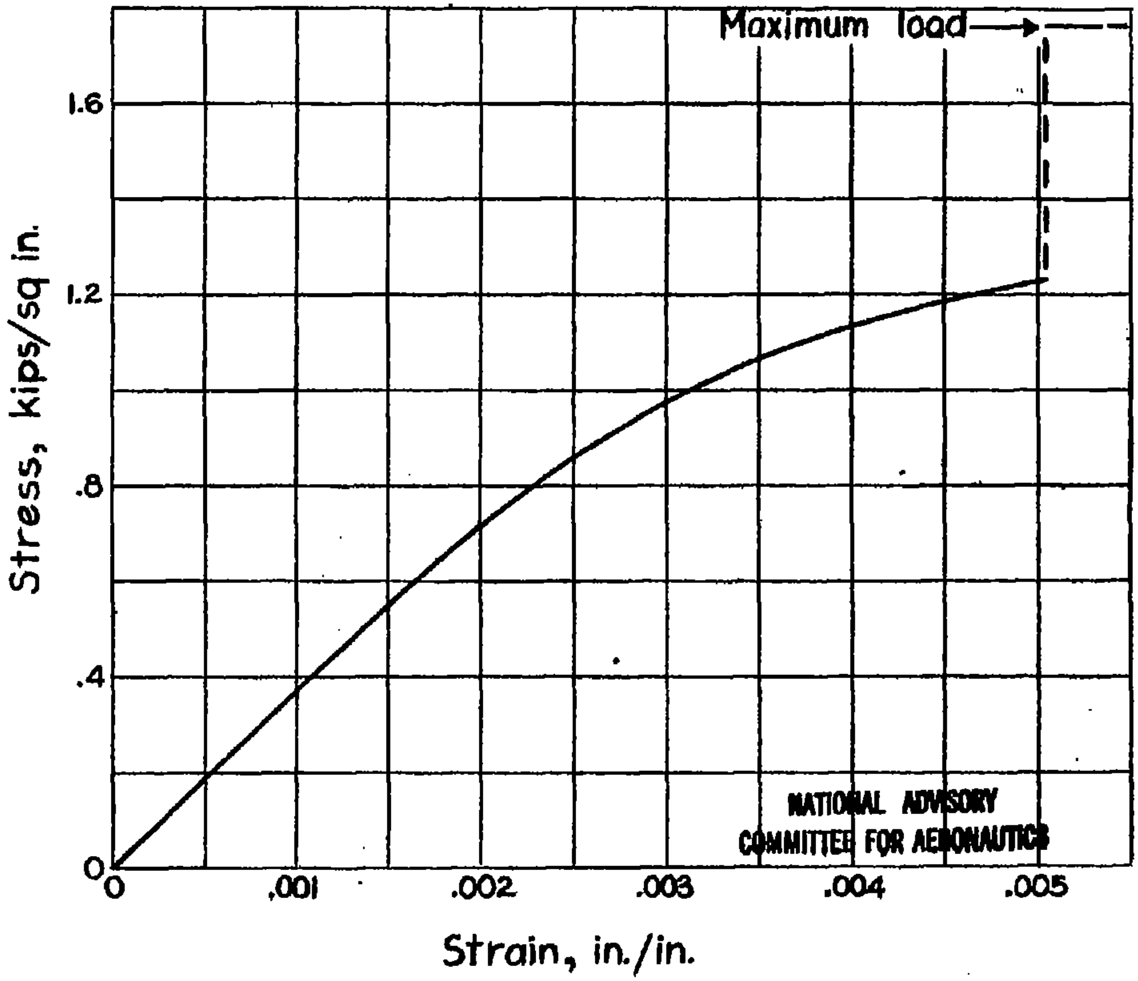

Figure 24. - Enlarged transverse tensile stress-strain curve for plastic-bonded unidirectional cloth.